CBN-05-4
February, 2005

Synchrotron-Light-Based Beam Profile Measurement in CESR

L.J. Antonelli[*], J.A. Crittenden and D.T. Kettler [†]
Cornell University

The synchrotron-light-based optical system used to measure the electron and positron vertical beam sizes has proved to be an essential diagnostic tool since the start of operations at CESR. Continuous immediate information on the behavior of the beams during both tuning and routine operation by means of television monitors as well as detailed analysis of profiles obtained with CCD arrays with long-term archiving provided useful information on emittance, instabilities and damping characteristics of the beams. The original telescopic optical system, which provided a resolution of about 170 microns, was complemented with a more accurate interferometric system in 2003. This note describes the relevant beam-line elements, the extraction of the light beam, the optical elements in the light path, and details of the associated control system.

1 Introduction

The installation of the six superconducting wiggler magnets during the summer of 2004 as part of the final phase of the CESR-c upgrade necessitated moving the synchrotron-light monitor for the electron beam from its position at 14W to the other available light port at 23W. The move motivated renewed effort to develop and document a detailed description of its design and operation. Taking advantage of this work, this note presents such a description of both the electron-monitoring system and the positron-monitoring system, which has been operating at 23E since the inception of CESR operations.

2 Optics

Figure 1 shows the optical light path of the synchrotron light extracted at 23W to monitor the electron beam. The system used for the positron beam at 23E is similar but for the absence of the two horizontal mirrors.

The synchrotron light beam sweeps across the beryllium mirror installed on the outer side of the beam pipe. The reflected light is extracted via the light port on the inner side of the beam pipe and enters the vertical periscope via a UV filter. The periscope contains two remotely controlled mirrors, the so-called “touchy” and “control” mirrors. Two horizontally reflecting fixed mirrors guide the light into the entrance of the optics box. The two horizontal mirrors outside the optics box, as well as the mirrors inside the box, are mechanically fixed and are cannot be adjusted remotely. The remotely controlled interferometer slits to be further described in

[*]Now at the University of Dallas, TX
[†]Now at the University of Washington, Seattle, WA

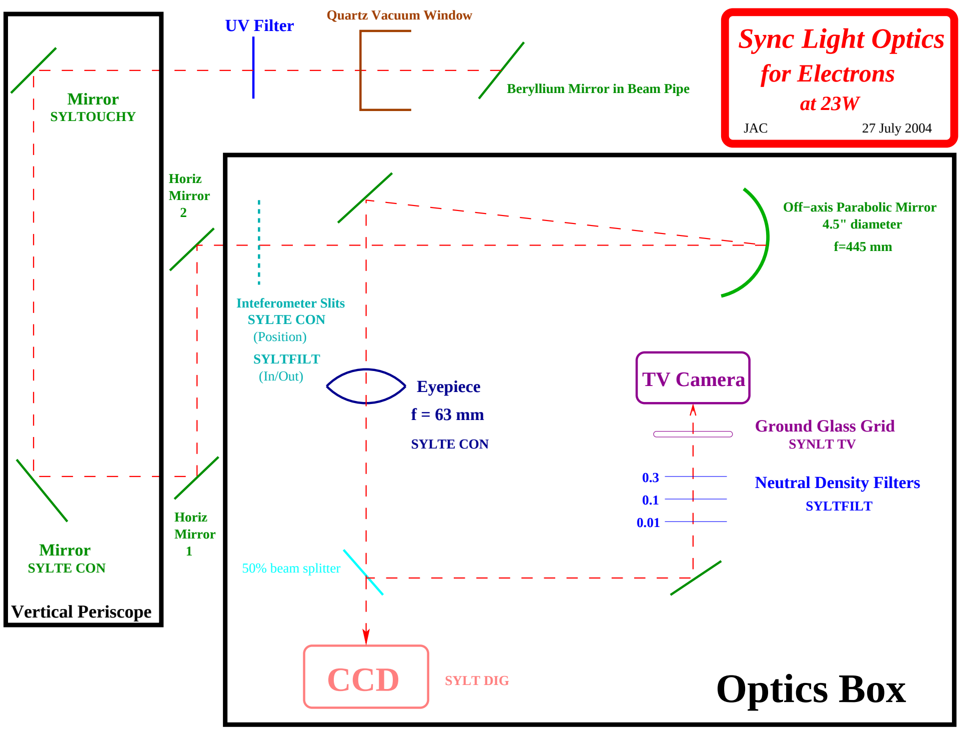

Fig. 1. Schematic diagram of the optical path of the synchrotron light extracted at 23W

Sect. 3 are located just inside the entrance to the optics box. The optical elements in the box act as a simple telescope. A parabolic mirror of 445-mm focal length focuses the image onto an eyepiece via one mirror. This eyepiece serves to focus on the light source point, which is inside the dipole magnet upstream of the primary mirror. The following splitter permits some of the light to continue onto a mirror which reflects it upward onto a CCD array. The rest of the light is reflected toward a TV camera via a set of remotely controlled neutral density filters.

Figure 2 shows the geometry of the synchrotron light extraction.[‡] P denotes the point of intersection between the line tangent to particle orbit at the end of the magnetic field and the line perpendicular to this tangent which intersects the extraction mirror location. The latter is the direction of the extracted light beam. The radius of the nominal central orbit is denoted by ρ; w is the distance from the end of the magnetic field to the point P; d is the distance from the point P to the extraction mirror; ϕ is half the arc angle along the particle orbit in the bend magnet from the light source point to the end of the magnetic field; $\alpha = 90 - \phi$; $\beta = 180 - 2\alpha = 2\phi$; γ is half the reflection angle at the extraction mirror; L is the distance from the light source point to the extraction mirror; $L' = L - \rho \sin \phi$.

Some simple relations based on the geometry follow:

$$L' = \frac{d}{\sin 2\phi}, \tag{1}$$

$$L = L' + \rho \sin \phi. \tag{2}$$

Since $d \ll \rho$, we make the following approximation:

$$L \approx \frac{d}{2\phi_0} + \rho\phi_0, \tag{3}$$

$$\rho\phi + w \approx \frac{d}{2\phi}, \tag{4}$$

$$\rho\phi + w \approx L', \tag{5}$$

$$\phi_0 \approx \left| \frac{-w - \sqrt{w^2 + 2\rho d}}{2\rho} \right|. \tag{6}$$

Introducing radial deviations from the nominal central orbit, x and x', we obtain:

$$L \approx \frac{d - x}{2\phi} + \rho(\phi - x'). \tag{7}$$

Typical values are $\rho = 89$ m, $w = 1.117$ m at 14W and $w = 1.457$ m at 23W, and $d = 4.5$ cm.

Figure 3 is the first application of Eq. 7, showing the distance from the source point to the mirror, L, as a function of the displacement x for several values of x'. This distance varies from 2.2 to 3.75 m at 14W and 2.4 to 3.9 m at 23W for pretzel

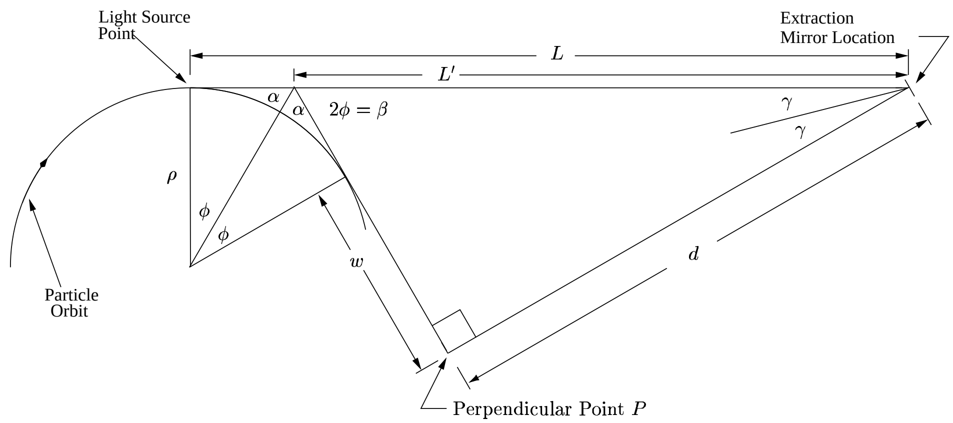

Fig. 2. Synchrotron light extraction geometry

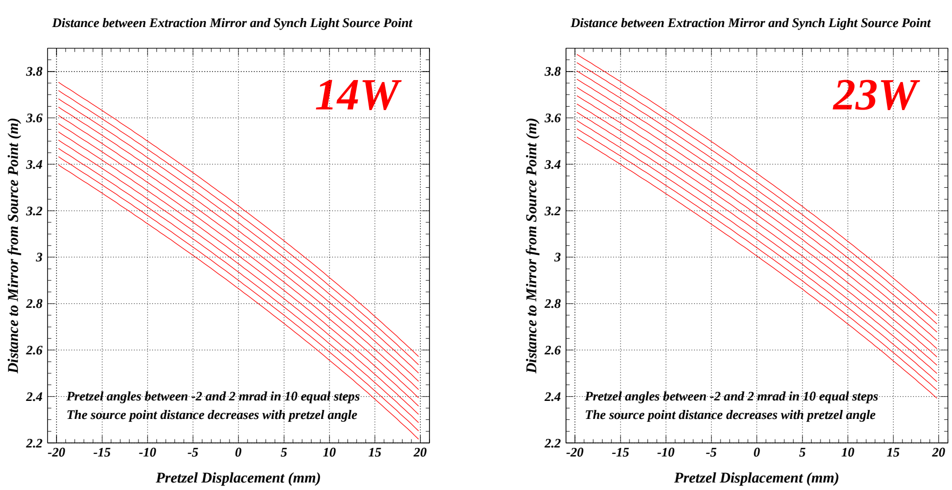

Fig. 3. Distance of the source point to the mirror for various pretzel angles at 14W and 23W

angles between −2 and 2 mrad and pretzel displacement between −20 and 20 mm. The difference in this distance between locations 14W and 23W is less than 20 cm.

The results of an analogous calculation is shown in Fig. 4, which gives the distance L for various values of x. L varies from about 1.75 to 3.65 m at 14W and 1.95 to 3.8 m at 23W for perpendicular distances from the mirror to the beam axis between 3 and 4.8 cm. The difference in this distance between locations 14W and 23W is less than 25 cm.

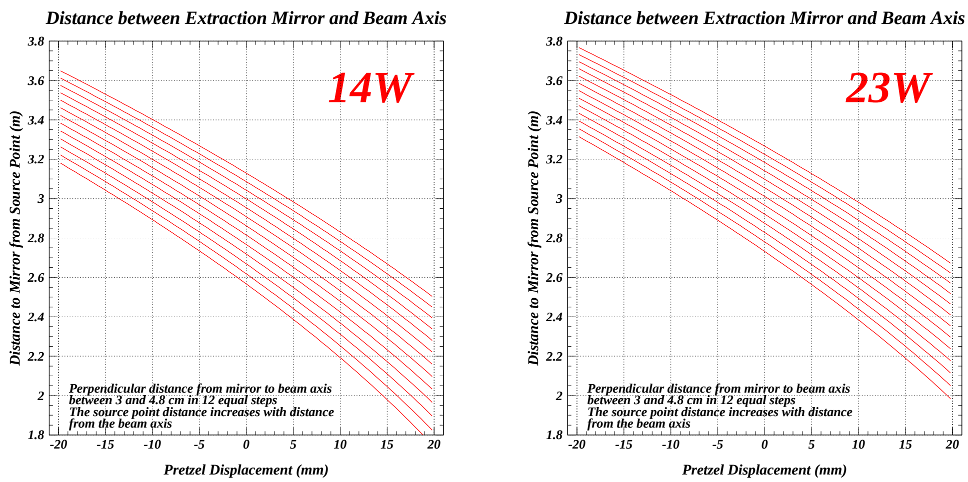

Fig. 4. Distance to the mirror for various perpendicular distances at 14W and 23W

Finally, Fig. 5 shows the extraction reflection angle as a function of pretzel displacement for 14W and 23W. This angle varies from .759 to .766 radians at 14W and .756 and .763 radians at 23W. The difference in this angle between locations 14W and 23W is less than 3 mrad.

The positions and lengths of the beam elements in 2004 are summarized in the following tables. Table 1 gives these values for 14W, Table 2 gives them for 23W, and Table 3 gives them for 23E.

Element	Distance of Element e^- Entrance from IP along e^+ flight direction (m)	Length (m)
e^- Mirror	93.622	0.0000
Bend Magnet B15W	101.300	6.5743
Quadrupole Q15W	102.057	0.60000
Sextupole X15W	102.394	0.27200

Table 1. Beam elements at 14W

‡See also S.V. Milton, M.S. thesis, Cornell University, 1988

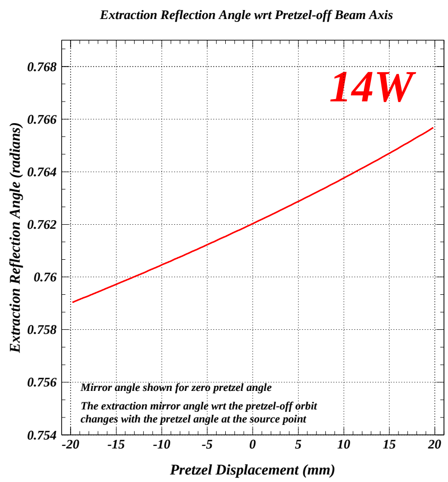

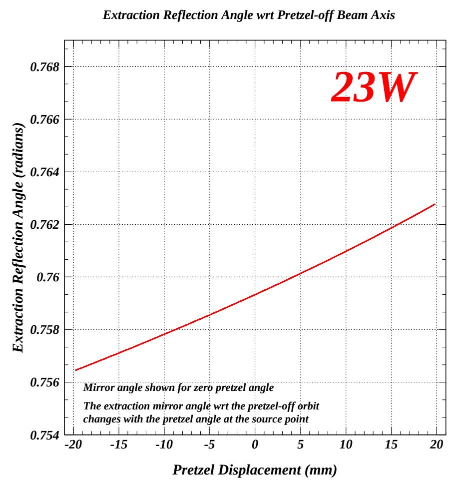

Fig. 5. Extraction reflection angle at 14W and 23W

Element	Distance of Element e^- Entrance from IP along e^+ flight direction (m)	Length (m)
e^- Mirror	167.553	0.00000
Bend Magnet B24W	175.601	6.5743
Quadrupole Q24W	176.358	0.60000
Sextupole X24W	176.830	0.27200

Table 2. Beam elements at 23W

Element	Distance of Element e^- Entrance from IP along e^+ flight direction (m)	Length (m)
Sextupole X24E	592.013	0.27200
Quadrupole Q24E	592.679	0.60000
Bend Magnet B24E	599.410	6.5743
e^+ Mirror	600.861	0.0000

Table 3. Beam elements at 23E

2.1 Optical Resolution

The two dominant contributions to the measurement of vertical beam size are the diffraction limit of about 100 microns and the depth-of-field of the optical system combined with the geometrical effect of the beam sweeping horizontally across the beryllium mirror, which contributes about 140 microns.[§]

The diffraction limit can be approximated as the apparent size of a point object viewed via the parallel component of polarization of the radiation in the visible region of the spectrum. The perpendicular component is filtered out in the optics. The RMS size of such an image is

$$\sigma_D \simeq \frac{1}{k\,\theta_0}, \tag{8}$$

where k is the wavenumber of the light ($\lambda = 2\pi/k = 500$ nm) and θ_0 is the vertical opening angle:

$$\theta_0 \simeq \left[\frac{\lambda}{2\pi^2\rho}\right]^{1/3} = 17\,\mu\text{rad}, \tag{9}$$

where ρ is the radius of curvature at the source point ($\rho = 89$ m). This opening angle is calculated in the approximation that the spectrum is limited to wavelengths much shorter than the critical wavelength of the synchrotron radiation.[¶] Note that the opening angle does not depend on the beam energy in this approximation, since the radius of curvature is fixed.

The contribution from the horizontal aperture limit A, which may be either the horizontal extent of the beryllium mirror, or an aperture in the optics further downstream, is

$$\sigma_f \simeq \frac{S}{2}\theta_0 \simeq \frac{A\rho}{2L}\theta_0, \tag{10}$$

where S is the length interval of the radiating particle trajectory from which light is accepted and L is the distance from the aperture limit to the source point.

The sum in quadrature of the two above contributions yields the total optical contribution of 170 microns to the measured vertical beam size.

2.2 Mirror-Alignment and Focusing Procedures

Two additional mirrors were required at 23W in the optical system by the longitudinal displacement of the optics box relative to the synchrotron light port. The primary beryllium mirror, the two mirrors in the vertical periscope, the new horizontal mirrors, the parabolic mirror in the optics box, and the mirror reflecting the beam onto the eyepiece, all had to be re-aligned.

[§] S.V. Milton, Master's thesis, Cornell University, 1988

[¶] *Electrodynamics*, J.D. Jackson, 2$^{\text{nd}}$ edition, p. 676

The beryllium mirror at 14W exhibited some thermal dis-coloration at the impact swath position of the synchrotron light, so it was replaced with a spare. The alignment of the new beryllium mirror was done by surveying the angle of the mount on the mounting port at 14W and by measuring the reflection angle relative to the mount in a bench setup prior to re-installing the mount on the mount port at 23W. Provision was made for a copper knife-edge vacuum seal ring which was to be manufactured on short notice at the time of installation to reproduce the mount angle at 14W. This turned out to be unnecessary, since the mount port at 23W turned out to have an angle relative to the beam axis close to that at 14W. However, the remounting of the beryllium mirror on its mount did turn out to be very important, since its angle was only approximately constrained by the mounting screws. So the procedure of fixing the mount, setting up a laser beam to measure the angle, removing the old mirror from the mount, then mounting the new mirror such as to reproduce this angle turned out to be crucial to the entire alignment procedure.

Once the beryllium mirror was installed, alignment of the downstream mirrors of the optical system required the use of an electron beam. Paper targets were set up sequentially at 1) the entrance to the vertical periscope to check the position and profile of the beam exiting the beampipe, 2) midway through the vertical periscope, 3) at the exit of the periscope, 4) midway between the horizontal mirrors, 5) in the optics box in front of the parabolic mirror, 6) in front of the eyepiece, and 7) at the 50% splitter in front of the CCD. For each position of the target, a TV camera was used to display in the control room the image of the synchrotron light beam on the target, borrowing the TV signal line connection at the electronics control rack for this purpose (see Fig. 7). Since each step required setting up the target and camera, then returning to the control room to see the position of the beam on the target, then returning to the tunnel to adjust the mirror position, then returning to the control room to check that the move had the desired effect, this procedure was very time-consuming. The complete alignment required three sessions of several hours each. With practice, aperture limits could be seen on the TV image of the beam profile. It was important to align each mirror in turn along the light path without skipping any steps. Viewing the target in front of the eyepiece involved aiming the camera through a separate port in the optics box and using a mirror inside the box for which the sole purpose was this step of the alignment procedure. Centering the beam on the eyepiece was useful, but since this is a focal point in the beam, it was the worst place to try to identify any shape to the profile such as would be caused by any aperture limits. The best place to see such structure was during the final step with the target in front of the beam splitter.

Once the mirrors were aligned, the source position as a function of eyepiece position was measured using an optical rail placed on top of the upstream dipole magnet. The collimated light-beam from a pen-lamp mounted on the rail was directed onto the entrance of a special-purpose two-mirror additional periscope set up so as to deflect the beam into the entrance port of the vertical periscope. Using a local TV monitor to view the beam image on the TV camera in the optics box, the source position at which the image was focused could be determined for several eyepiece position settings. This eyepiece position setting was measured locally with a DVM on the local control chassis (see Fig. 7). The calibration of readback voltage to control database computer units (f) was then obtained to determine the following functions for source point (distance from the interaction point) and magnification factor:

23W e^-	Source Point (m) $= (170.076 + 0.220) - (f - 560) * 0.004$ Magnification $= 1 + (f - 800) * 0.0008$
23E e^+	Source Point (m) $= (597.60 + 0.220) + (f - 600) * 0.004$ Magnification $= 1 + (f - 700) * 0.0008$

The magnification is defined here as the size of the TV image divided by the collimated source size. The contribution of the length of the special-purpose periscope, 22 cm, is shown explicitly in the calculation. The settings of the eyepiece position as of October, 2004, were $f = 520$ for the positron beam, resulting in a source position of 597.50 and a magnification factor of 0.86. For the electron beam, the setting was $f = 422$, yielding a source position of 170.85 and a magnification of 0.70.

3 Interferometer

Interferometer slits can be dropped into the synchrotron-light beam at the entrance port of the optics box, providing a means for measuring the transverse image size avoiding the optical sources of resolution which amount to about 170μ for the imaging method described in this note. The slits of the interferometer are 500 μ wide and spaced 2 mm apart. There is a filter in front of the interferometer slits which transmits a 10 nm wide optical frequency band centered at 500 nm. The interference pattern is imaged with the CCD array and analyzed off-line to provide accurate measurements of the vertical beam size. Figure 6 shows an example of such an interference pattern. This intensity pattern is given by

$$I(x) = I_0 \left[\frac{\sin \frac{2\pi w x}{f\lambda}}{\frac{2\pi w x}{f\lambda}} \right]^2 \left(1 + V \cos \frac{2\pi d x}{\lambda} \right), \tag{11}$$

where w is the slit width, d is the slit spacing, λ is the frequency of the light, f is the distance from the grid to the image (about 1.5 m), and V is the "visibility" parameter, which is a measure of the ability of the system to determine the source size. This visibility parameter is given by

$$V = \exp \left[-2 \left(\frac{\pi d\, \sigma_{\rm beam}}{\lambda L} \right)^2 \right], \tag{12}$$

where L denotes the distance of the source from the grid (about 5 m) and σ_{beam} is the RMS transverse size of the source.

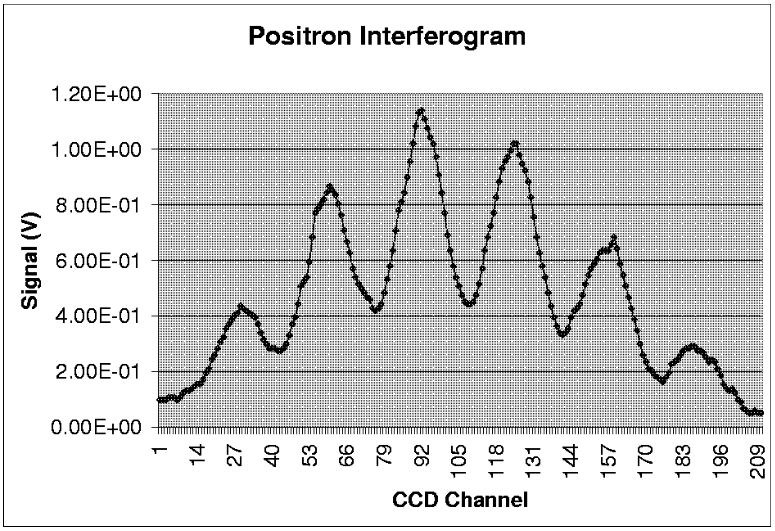

Fig. 6. Example of an interference pattern produced with the interferometer

4 Control and Readback Electronics

The control and readback electronics of the system are mounted in half-height racks on the tunnel floor near 23E and 23W. The main parts of the system that need electronic control are the upper ("touchy") and lower ("control") mirrors in the vertical periscope, the eyepiece, the interferometer slits, the optical filters, and the CCD camera. Figure 7 shows a diagram of the local electronics rack at 23W. The functions for the various control parameters are given in Table 4. The control database mnemonics are also shown. These controls are found in the control system database under HEP TUNING/CSR DIAGNOSE. Figure 9 shows the corresponding entries in the database. The insertion switches for the optical filters and the interferometer slits are found in rack CRB.10 in the control room. A diagram of the connections in the patch panel on the bottom of the optics box at 23W is shown in Fig. 8. There is in addition a second flat cable feedthrough on the side of the optics box which carries control signals for the CCD.

5 Summary

The installation of the electron synchrotron-light apparatus at 23W took place during the four-month shutdown which ended in August, 2004. Mirror alignment and source-point measurements were performed during the weeks following

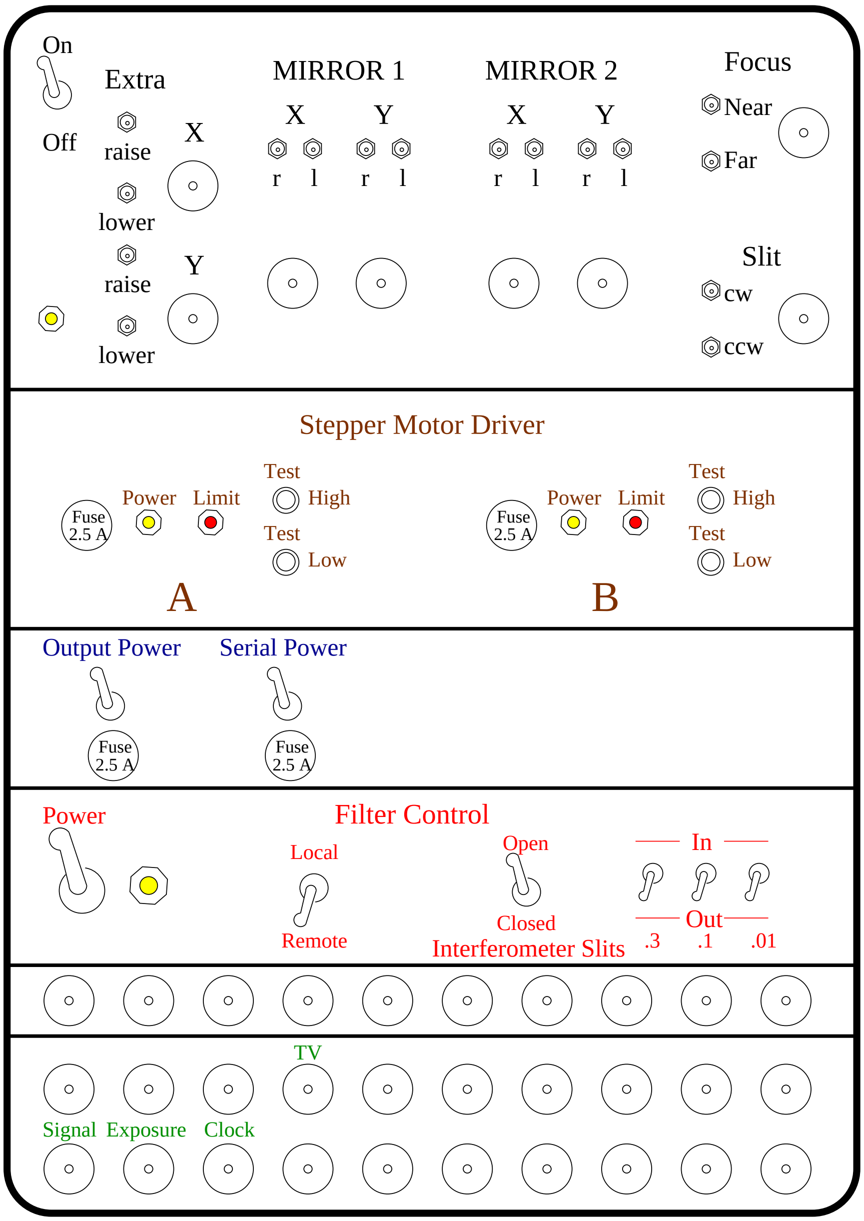

Fig. 7. Diagram of electronics control rack at 23W

Element Label		Device Controlled	Purpose of Element	Database mnemonic
X	raise	Top mirror	tilts mirror right	CSR SYLTOUCHY
	lower		tilts mirror left	CSR SYLTOUCHY
X	raise	Bottom mirror	tilts mirror right	CSR SYLTE CON
	lower		tilts mirror left	CSR SYLTE CON
Y	raise	Top mirror	tilts mirror up	CSR SYLTOUCHY
	lower		tilts mirror down	CSR SYLTOUCHY
Y	raise	Bottom mirror	tilts mirror up	CSR SYLTE CON
	lower		tilts mirror down	CSR SYLTE CON
Near		Eyepiece	moves source point nearer	CSR SYLTE CON
Far			moves source point further	CSR SYLTE CON
cw		Interferometer Slits	rotates slits clockwise	CSR SYLTE CON
ccw			rotates slits counterclockwise	CSR SYLTE CON
Local/Remote		Optical Filters	toggles control to control room	
Interferometer slits		Interferometer slits	inserts/removes slits	CSR SYLTFILT
0.3		0.3 optical filter	inserts/removes filter	CSR SYLTFILT
0.1		0.1 optical filter	inserts/removes filter	CSR SYLTFILT
0.01		0.01 optical filter	inserts/removes filter	CSR SYLTFILT
Signal		CCD Camera	Output signal	
Expo			Exposure control	
Clock			obsolete	
TV		TV Camera	TV camera output signal	

Table 4: Local controls on the control rack at 23W shown in Fig. 7. Only the mirrors in the vertical periscopes are controlled. The corresponding control database entries can be found in the Fig. 9 and in the diagram of the optics box in Fig. 1. These controls are found in the control system database under HEP TUNING/CSR DIAGNOSE.

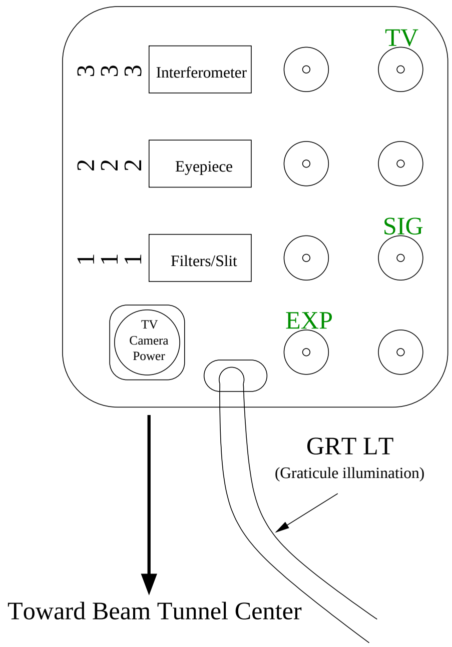

Fig. 8. Diagram of control cable patch panel on the bottom of the optics box viewed from below

re-commissioning of CESR operation. During the first couple of weeks following this startup, some significant motion of the electron synchrotron-light image was observed, requiring periodic readjustment of the mirrors in the vertical periscope. This apparent motion of the beam pipe stabilized on the time scale of a few weeks.

Acknowledgments

We wish to acknowledge invaluable discussions with Don Hartill, Mike Billing and John Sikora. Mike also did a critical reading of this note. Mark Palmer provided the example of an interferometer intensity pattern. Scott Chapman performed the survey work and the beryllium mirror alignment. John Barley and Mike Comfort took care of moving the readout and control electronics from 14W to 23W. LJA received support from the Research for Undergraduates program funded by the National Science Foundation.

```
n       'CSR SYLT DIG' 18   20  18000000 82838701 8 0 0 0 4 0 15 0  11!
c        cmd wrraw-shf-msk wrmode stat tim  xberrad str xbout-errtim
f       8h a16 2h
e        0 0 0 3  4 0 0 0   'E- SYNLIT MODE  ' C17950 0!  1 mode
e        0 0 2 F  4 0 0 0   'E- SYNLIT CLOCK ' C17950 0!  2 clock speed
e        0 0 6 F  4 0 0 0   'E- SYNLIT INTEG ' C17950 0!  3 integ frames
e        0 0 0 ffff 0 0 0 0 'E- SYNLIT WORD  ' C17950 0!  4 all UNSHARED
e        0 0 0 0  0 0 0 0   '                ' 000000 0!  5
e        0 0 0 0  0 0 0 0   '                ' 000000 0!  6
e        0 0 0 0  0 0 0 0   '                ' 000000 0!  7
e        0 0 0 0  0 0 0 0   '                ' 000000 0!  8
e        0 0 0 0  0 0 0 0   '                ' 000000 0!  9
e        0 0 0 0  0 0 0 0   '                ' 000000 0! 10
e        0 0 0 3  4 0 0 0   'E+ SYNLITMODE   ' b17950 0! 11
e        0 0 2 F  4 0 0 0   'E+ SYNLIT CLOCK ' B17950 0! 12
e        0 0 6 F  4 0 0 0   'E+ SYNLIT INTEG ' B17950 0! 13
e        0 0 0 ffff 0 0 0 0 'E+ SYNLIT WORD  ' b17950 0! 14
e        0 0 0 0  0 0 0 0   '                ' 000000 0! 15
e        0 0 0 0  0 0 0 0   '                ' 000000 0! 16
e        0 0 0 0  0 0 0 0   '                ' 000000 0! 17
e        0 0 0 0  0 0 0 0   '                ' 000000 0! 18
e        0 0 0 0  0 0 0 0   '                ' 000000 0! 19
e        0 0 0 0  0 0 0 0   '                ' 000000 0! 20

n        'CSR SYLTFILT' 18    8  18000000 80838701 8 0 0 0 4 0 15 0  10!
c        cmd wrraw-shf-msk wrmode stat tim  xberrad xbout-errtim
f       10h
e        0 0 F 1  0 0 0 0 C17068 0!  1
e        0 0 F 1  0 0 0 0 C17069 0!  2
e        0 0 F 1  0 0 0 0 C1706A 0!  3
e        0 0 F 1  0 0 0 0 C1706B 0!  4
e        0 0 F 1  0 0 0 0 B16068 0!  5
e        0 0 F 1  0 0 0 0 B16069 0!  6
e        0 0 F 1  0 0 0 0 B1606A 0!  7
e        0 0 F 1  0 0 0 0 B1606B 0!  8
n        'CSRSYLTOUCHY'  2    4  28000000 D3F7E7CF 8 0 0 5 4 11 15 0  25!
c        cmd old val rdraw-off-sca  wrraw-shf-msk-llm-ulm-mode
c        sts tim dly limrd-bit cmdinc xberrad c  rdmap strptr xbin-lim-out-errtim
f        5i f i 2h 2i h 4i 4h a16 4h
e        0 0 0 0 0 0.5 0 0 FFFFFFFF -1000 1000 2 1 0 390 0 0 F 0 1 'E- HORZNTAL TILT' d1d516 0 d1d000 0!  1
e        0 0 0 0 0 0.5 0 0 FFFFFFFF -1000 1000 2 1 0 390 0 0 F 0 1 'E- VERTICAL TILT' d1d518 0 d1d002 0!  2
e        0 0 0 0 0 0.5 0 0 FFFFFFFF -1000 1000 2 1 0 390 0 0 F 0 1 'E+ VERTICAL TILT' B16058 0 B17600 0!  3
e        0 0 0 0 0 0.5 0 0 FFFFFFFF -1000 1000 2 1 0 390 0 0 F 0 1 'E+ HORZNTAL TILT' B16059 0 B17602 0!  4
c
n        'CSRSYLTE CON'  2    8  20000000 D3F7E7CF 8 0 0 5 4 11 15 0  25!
c        cmd old val rdraw-off-sca  wrraw-shf-msk-llm-ulm-mode
c        sts tim dly limrd-bit cmdinc xberrad c  rdmap strptr xbin-lim-out-errtim
f        5i f i 2h 2i h 4i 4h a16 4h
e        5(0) 0.5 0 0 FFFFFFFF -1000 1000 2 1 0 390 0 0 F 0 1 'E- HORZNTAL TILT' d1d51a 0 d1d004 0!  1
e        5(0) 0.5 0 0 FFFFFFFF -1000 1000 2 1 0 390 0 0 F 0 1 'E- VERTICAL TILT' d1d51c 0 d1d006 0!  2
e        5(0) 0.5 0 0 FFFFFFFF -1000 1000 2 1 0 390 0 0 F 0 1 'E- FOCUSING     ' d1d51e 0 d1d008 0!  3
e        5(0) 0.5 0 0 FFFFFFFF -1000 1000 2 1 0 390 0 0 F 0 1 'INTERFEROMETER  ' d1d520 0 d1d00A 0!  4
```

```
e       5(0) 0.5 0 0 FFFFFFFF -1000 1000 2 1 0 390 0 0 F 0 1 'VRT SLIT (LOWER)' d1d522 0 d1d00C 0!  5
e       5(0) 0.5 0 0 FFFFFFFF -1000 1000 2 1 0 390 0 0 F 0 1 'VRT SLIT (UPPER)' d1d524 0 d1d00E 0!  6
e       5(0) 0.5 0 0 FFFFFFFF -1000 1000 2 1 0 390 0 0 F 0 1 ' SPARE          ' d1d526 0 d1d010 0!  7
e       5(0) 0.5 0 0 FFFFFFFF -1000 1000 2 1 0 390 0 0 F 0 1 ' SPARE          ' d1d528 0 d1d012 0!  8
c
c       newnode for syn light graticule illumination
n       'CSR SYNLT TV'  1   2  20000000 93C7F9CF 8 0 0 5 6 11 16 0  22!
c       cmd old val rdraw-off-sca  wrraw-off-sca-llm-ulm-mode
c       sts tim dly cmdinc xberrad rdmap  strptr xbin-out xberrtim
f       5i f 2i f 6i 3h a16 3h
e       5(0) 1.0 0 0 1. 0 1600 0 1 4(0) 1 'E+ GRID ILUM 23E' d1961a d19702 0!  1
e       5(0) 1.0 0 0 -4. 0 511 0 1 4(0) 1 'E- GRID ILUM 23W'      0 d1D702 0!  1
c
n       'CSRSYLTP CON'  2    6  08000000 D3F7E7CF 8 0 0 5 4 11 15 0  25!
c       cmd old val rdraw-off-sca  wrraw-shf-msk-llm-ulm-mode
c       sts tim dly limrd-bit cmdinc xberrad c  rdmap strptr xbin-lim-out-errtim
f       5i f i 2h 2i h 4i 4h a16 4h
e       5(0) 0.5 0 0 FFFFFFFF -1000 1000 2 1 0 390 0 0 F 0 1 'E+ HORZNTAL TILT' B1605A 0 B17604 0!  1
e       5(0) 0.5 0 0 FFFFFFFF -1000 1000 2 1 0 390 0 0 F 0 1 'E+ VERTICAL TILT' B1605B 0 B17606 0!  2
e       5(0) 0.5 0 0 FFFFFFFF -1000 1000 2 1 0 390 0 0 F 0 1 'E+ FOCUSING     ' B16018 0 B17608 0!  3
e       5(0) 0.5 0 0 FFFFFFFF -1000 1000 2 1 0 390 0 0 F 0 1 'INTERFEROMETER  ' B16019 0 B1760A 0!  4
e       5(0) 0.5 0 0 FFFFFFFF -1000 1000 2 1 0   0 0 0 F 0 1 'VRT SLIT (LOWER)'  0 0 B1760C 0!  5
e       5(0) 0.5 0 0 FFFFFFFF -1000 1000 2 1 0   0 0 0 F 0 1 'VRT SLIT (UPPER)'  0 0 B1760E 0!  6
c
c  NEW NODE TO CONTROL SYNCH LIGHT INTEGRATION TIME
n       'CSR SYLT INT' 18    8  10000000 82838701 8 0 0 0 4 0 15 0  11!
c       cmd wrraw-shf-msk wrmode stat tim  xberrad STRPTR xbout-errtim
f       8h A16 2H
e       0 0 F 1  0 0 0 0  '                '  000000 0!  1 (LSB?)
e       0 0 F 1  0 0 0 0  '                '  000000 0!  2
e       0 0 F 1  0 0 0 0  '                '  000000 0!  3
e       0 0 F 1  0 0 0 0  '                '  000000 0!  4 (MSB?)
e       0 0 F 1  0 0 0 0  '23E E+ SL INT B0'  B17028 0!  5
e       0 0 F 1  0 0 0 0  '23E E+ SL INT B1'  B17029 0!  6
e       0 0 F 1  0 0 0 0  '23E E+ SL INT B2'  B1702A 0!  7
e       0 0 F 1  0 0 0 0  '23E E+ SL INT B3'  B1702B 0!  8
```

Fig. 9. Control database entries